Electronic structure of YFe2 by EELS and ab-initio calculations

E- Yáñez-Terrazas, V. Gallegos-Orozco, J.A. Matutes-Aquino, M.T. Ochoa-Lara, and F. Espinosa-Magaña.

Abstract

The dielectric properties of the intermetallic cubic Laves phase compound YFe2 were determined by analyzing the low loss region of the EELS spectrum in a transmission electron microscope. From these data, the optical joint density of states (OJDS) was obtained by Kramers-Kronig analysis. Since maxima observed in the OJDS spectra are assigned to interband transitions; these spectra can be interpreted on the basis of numerical calculations performed with the Wien2k code, using the Fully-Linearized-Augmented-Plane wave (FLAPW) method within the Local-Spin-Density Approximation. Comparison between experimental results and theory shows good agreement

Keywords: EELS; Dielectric Function; YFe2; Electronic Structure.

Introduction

The study of rare-earth transition-metal (RE–TM) intermetallic compounds and the detailed description of their magnetic behavior present many interesting aspects. Yttrium-transition metal (Y–TM) are prototypes for RE–TM compounds, because yttrium is chemically very similar to the trivalent rare-earth atoms and thus allowing a band structure (BS) calculation for these compounds as a consequence of not having a partially filled 4f-shell [1]. The wide range of intermetallics with different stoichiometries and with different rare-earth elements in them allows the systematic research of their magnetic properties and complex interactions between *3d-4f* electrons. The cubic Laves

phase structure compounds form a wide class of magnetic materials with important applications, being the rare earth-iron (RE-Fe_2) based materials to be known as possessing interesting magnetic properties associated with 3d electrons in Fe atoms. The basic separation of the localized 4f and the itinerant *3d* electrons allows one to consider the high T_C and the anisotropy of these itinerant ferromagnets as a consequence of the strong exchange Fe–Fe and Fe–RE interaction, respectively, being the latter due to the strong spin-orbit coupling experienced by the 4*f* electrons [2, 3].

In this work we calculate the electronic structure and density of states of the intermetallic cubic Laves phase compound YFe_2 with the WIEN2k code, using the Fully-Linearized-Augmented- Plane-Wave (FLAPW) method within the Local-Spin-Density-Approximation (LSDA). The results obtained from the band structure calculations and the density of states are supported with experimental data obtained from Electron Energy Loss Spectroscopy (EELS) technique in the transmission electron microscope (TEM). We carried out an analysis in the low energy loss region of the spectrum and a comparison is made between theory and experiment. Kramers-Kronig analysis is performed to obtain the complex dielectric function from spectroscopic data.

Electron energy-loss spectroscopy (EELS) is a powerful analytical technique that can be utilized to obtain information on the structure, bonding and electronic properties of a material [4-10]. The interactions of fast electrons with the specimen result in excitations of electrons into unoccupied energy levels in the conduction band. When a spectrum is obtained by analyzing the energy lost by the incident electrons, the region up to an energy loss of ~50 eV is dominated by collective excitations of valence

electrons (plasmon) and by interband transitions. At higher energy losses ionization edges occur due to excitation of core electrons into the conduction band.

To our knowledge, combined EELS and *ab initio* calculations have not been used for studies of YFe_2 yet. In the present work we have conducted low-energy EELS on arc-melting prepared YFe_2 samples obtaining the complex dielectric function and the optical joint density of states by Kramers-Kronig analysis.

The low loss region in an energy loss spectrum (<50 eV) contains information about excitations of outer shell electrons and the electronic structure of the material which determines its optical properties. The excitations of valence electrons are dominated by collective excitations (plasmon) and single electron interband transitions. Interband transitions are originated from the excitation of electrons to empty states in the conduction bands, so these can be identified as transitions in a band structure model.

From the dielectric theory, it is possible to relate the experimental single scattering distribution S(E), to the Energy Loss Function Im(-1/ε), by [8]:

$$S(E) = \frac{I_0 t}{\pi a_0 m_0 v^2} \mathrm{Im}\left[-\frac{1}{\varepsilon(q,E)}\right] \ln\left[1 + (\beta/\theta_E)^2\right] \qquad (1)$$

where ε(q,E) = ε1+ iε2 is the complex dielectric function at energy loss E and momentum transfer q, a_0 the Bohr radius, m_0 the electron rest mass, v the electron beam velocity, na the number of atoms per unit volume, q the scattering angle and θ_E = $E/(ym0v^2)$ is the characteristic scattering angle, g is the relativistic factor, I0 is the zero loss intensity, t is the specimen thickness and b is the collection semi-angle.

To compare the experimental results from EELS with the density of states (DOS) obtained from band theory calculations, we can define the optical joint density of states (OJDS), as [10,11]

$$J_1(E) = \frac{2E\varepsilon_2(E)}{\pi E_p^2} \qquad (2)$$

where E_p is the plasmon energy in Drude model.

Experimental details

The samples were prepared by arc melting from the pure elements, Y (99.9%) and Fe (99.98%), under an argon atmosphere. Buttons were prepared and sealed in an evacuated quartz tube, then annealed for 90 h at 850°C and quenched in cold water. To avoid the risk of having undesirable phases in the initial samples, a thin layer was filed off from the surface of the buttons.

EELS spectra were taken in diffraction mode with 0.2 eV/ch dispersion, an aperture of 2 mm and a collection semi-angle of 2.7 mrad. The resolution of the spectra was determined by measuring the full width at half-maximum (FWHM) of the zero-loss peak and this was typically close to 1.3 eV when the TEM was operated at 200 kV. Spectra were corrected for dark current and readout noise. The channel to channel gain variation was minimized by normalizing the experimental spectrum with independently obtained gain spectrum of the spectrometer.

Calculation Details

Self-consistent band structure calculations were performed using density functional theory (DFT) with the full-potential linearized augmented plane-wave

(FLAPW) method using the WIEN2k code [12]. Exchange and correlation were treated using the Local-Spin-Density Approximation (LSDA) for the potential. The core states were treated in a fully relativistic fashion. The wave functions within the muffin-tin spheres were expanded in spherical harmonics with an angular momentum up to l = 10. Additional local orbital extensions were used to avoid linearization errors. Nonspherical contributions to the charge density and the potential within the muffin-tin spheres were considered up to l_{max} = 4. In the interstitial region, plane waves with reciprocal lattice vectors up to G = 10 were included and the plane-wave cut-off ($R_{MT}K_{max}$) was set to 8. For this compound, the muffintin radii were chosen as 2.50 and 2.44 a.u. for Y and Fe respectively. Self-consistency was considered to be achieved when the total energy variation from iteration to iteration did not exceed 10^{-5} Ry, on a mesh containing 165 k-points in the irreducible Brillouin zone (IBZ).

The dielectric function can be obtained from the OPTIC Program of the WIEN2k code, Ambrosch et al. [13] , allowing for comparison with experiment:

$$\varepsilon_{2ii}(\omega) = \frac{4\pi^2 e^2}{m^2\omega^2 V}\sum_{v,c,k}\left|\left\langle\psi_k^v\left|p_i\right|\psi_k^c\right\rangle\right|^2 \times \delta\left(E_{\psi_k^c} - E_{\psi_k^v} - \hbar\omega\right) \quad (3)$$

Matrix elements are calculated from the electron states and an integration over the irreducible Brillouin zone is performed to calculate the imaginary part of the dielectric function and then a Kramers-Kronig analysis is performed to obtain the real part of the dielectric function ε1 and finally the energy loss function Im(-1/ε). The optical properties were calculated on a mesh containing 1540 k-points in the irreducible part of the Brillouin zone, as many points are needed for optical calculations.

The crystal structure of YFe_2 has been widely studied experimentally. This is a cubic structure and belongs to the space group Fd-3m. The lattice constant is 7.362 Å, taken from the experimental results [14]. The atomic positions are: Y at (0,0,0) and Fe at (0.625,0.625,0.625).

Results and Discussion

Spectra acquired with the EELS spectrometer were Fourier-Log deconvoluted to have the single scattering distributions S(E), and then normalized to obtain the energy loss function Im(-1/ε). The real and imaginary parts of the dielectric function were obtained, after removing surface loss effects, by Kramers-Kronig Analysis, as described by Egerton [8].

The energy loss function and the real part of the dielectric function are shown in Fig. 1. The ε1 spectrum shows zero upward crossing at 16.0 eV, indicating that the dominant peak in the energy loss spectrum at 16.8 eV is a well defined plasmon and peak at 25.8 eV corresponds to Y N_{23} ionization edge. The absence of any other zero crossing implies that other featured peaks appearing at energies below the plasmon peak are effectively due to interband transitions. As peak positions in the energy loss spectrum at low energy losses are strongly influenced by the volume plasmon and the positions of other excitations, the energy loss spectrum cannot be directly associated with interband transitions. However, the imaginary part of the dielectric function can be associated with interband transitions. Fig. 2 shows the imaginary part of the dielectric function. At first sight, no structure is observed in the spectrum; however, this structure exists and it can be made evident by calculating the optical joint density of states $J_1(E)$, from Eq. (2). Fig. 3 shows a plot of $J_1(E)$ Vs E, where some structure has been

appeared. Taking the second derivative of $J_1(E)$ with respect to E, the structure in the $J_1(E)$ Vs E plots are further enhanced, as it is shown in Fig. 4. Peaks not visible in the $J_1(E)$ Vs E plots show relative maxima in $-d^2J1(E)/dE^2$ Vs E plots. The appearance and height of these peaks show clearly that they are not noise in character, showing instead more structure associated with interband transitions. However, it should be stressed that wiggles in the second derivative of the OJDS have no physical meaning but are just a mathematical procedure to enhance the structure not visible, at first sight, in the OJDS Vs E plot. On the other hand, peak positions in the derivative correspond with peaks positions in OJDS and the OJDS is proportional to the joint density of states (JDOS) [11,15]. The electronic structure information available in the low-loss EELS spectrum is related to the joint density of states which is high for energies at which two energy surfaces lie parallel to one another at a particular k point in reciprocal space. At such points one has the so-called critical points. As single electron interband transitions depend on critical points in the band structure, peaks in the imaginary part of the dielectric function come from to the presence of critical points in the band structure.

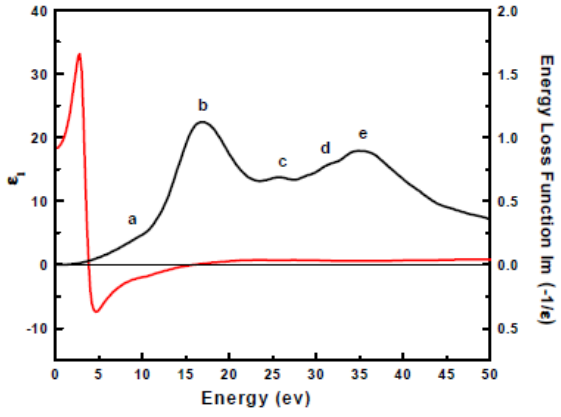

Fig. 1. EELS obtained Energy Loss Function Im(-1/ε), and real part of the dielectric function ε_1.

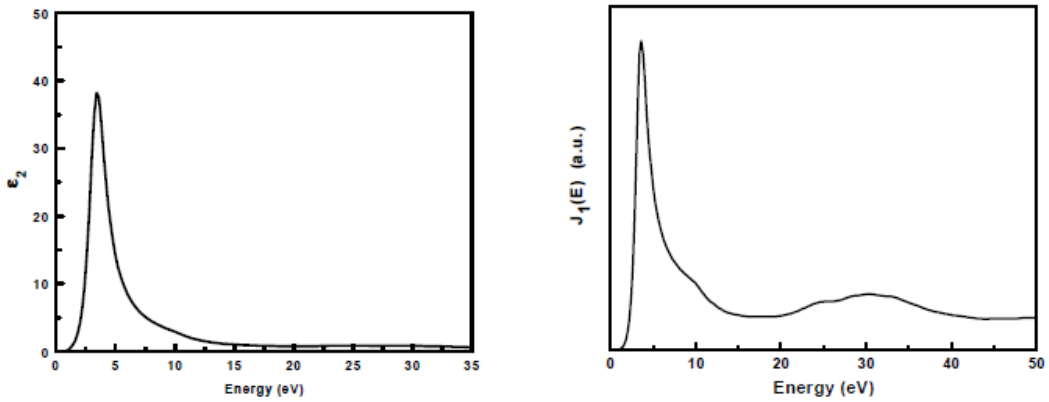

Fig. 2. (left) EELS obtained imaginary part of the dielectric function ε_2., Fig. 3.(right) Kramers-Kronig derived optical joint density of states $J_1(E)$.

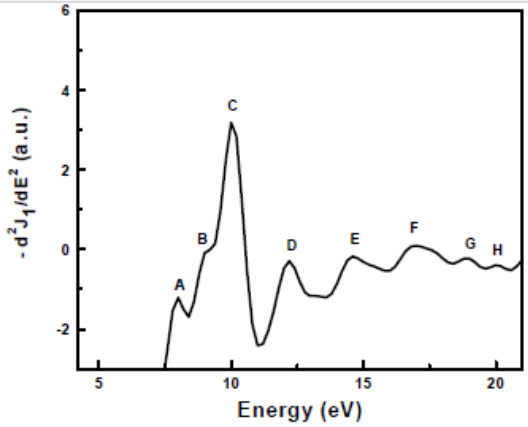

Fig. 4. Second derivative of the Optical Joint Density of states.

As maxima observed in the $J_1(E)$ Vs. E plots are assigned to interband transitions, these peaks can be interpreted on the basis of energy-band calculations. Figs. 5, 6 show the calculated energy loss function and the imaginary part of the dielectric function ε2, respectively, where we chose not to broaden these quantities, as it is well known that experimental broadening is a much more complex process. Featured peaks a-e in Fig. 1 for the experimental energy loss function, coincide well

with corresponding peaks in Fig. 5 from theoretical calculations, as long as energy positions of relative maxima are concerned, even though a lack of absolute intensity in the theoretical calculations is observed when compared to experiments. In the same way, we find good coincidence between featured peaks A-H in Fig. 4, arising from experimental results and those observed in Fig. 6 for the calculated imaginary part of the dielectric function.

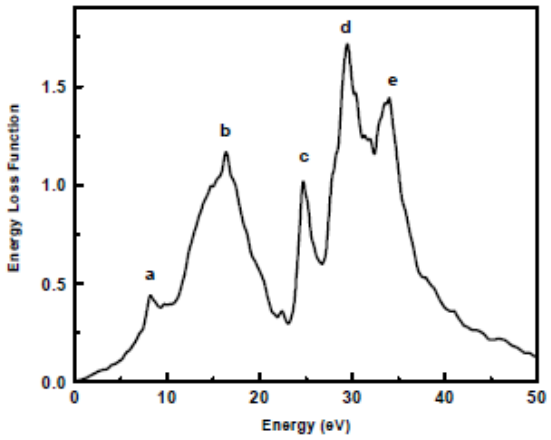

Fig. 5. Calculated energy loss function Im(-1/ε) for YFe_2

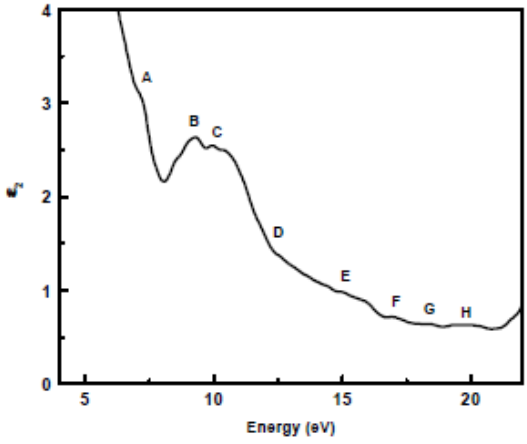

Fig. 6. Calculated imaginary part of the dielectric function for YFe_2

As long as the magnetic properties are concerned, we calculated the spin-dependent density of states. Fig. 7 shows the density of states for spin-up and spin-down electrons for the compound YFe_2, as well as the partial density of states for Y and Fe sites, from numerical calculations. From these plots, it is evident that the ferromagnetic character for YFe_2 comes mainly from Fe. Actually, total magnetic moment in the unit cell, from calculations, comes out to be 3.68 μB, with Y sites giving a small negative contribution to the total magnetization of 0.09 μB, in agreement with calculations performed with different methods [16]. Our calculated magnetic moment per unit cell comes out to be higher than reported experimental values of 2.90 μB and 2.86 μB calculated by other authors [17, 18].

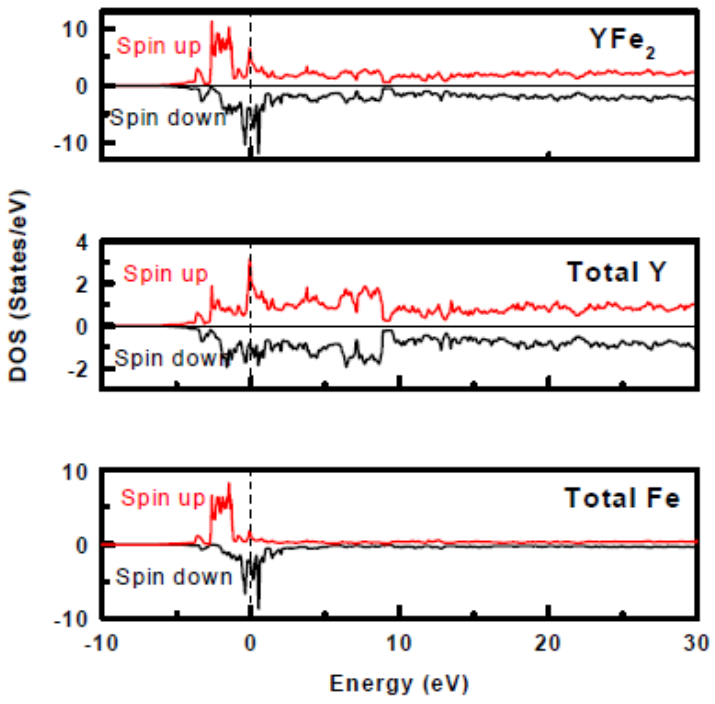

Fig. 7. Calculated total and partial density of states.

Conclusion

Electronic structure of YFe_2 samples was studied by low-loss transmission Electron Energy Loss Spectroscopy. We obtained Kramers-Kronig derived complex dielectric function and optical joint density of states (OJDS) for YFe_2. Peaks in the OJDS were enhanced by taking the second derivative with respect to energy loss and compared with numerical calculations. Good agreement was found between our experimental results and those based on theoretical calculations.

References

[1] N. Nakada, H. Shimizu, H. Yamada, Physica B 329-333 (2003), p. 1129

[2] C. Ritter, J. Phys.: Cond. Matter. 1 (1989), p. 2765

[3] H. Yamada, J. Inoue, K. Terao, S. Kanda, M. Shimizu, J. Phys. F: Met. Phys. 14 (1984), 1943

[4] R.H. Ritchie, Phys. Rev. 106 (1957), p. 874

[5] J. Daniels, C.V. Festenberg, H. Raether, K. Zeppenfeld. Optical Constants of Solids by Electron Spectroscopy. Springer Tracts in Modern Physics, Springer-Verlag, New York; (1970), Vol. 54, p. 78-135

[6] H. Raether. Excitation of Plasmons and Interband Transitions by Electrons. Springer Tracts in Modern Physics Vol 88, Springer-Verlag New York (1980)

[7] K. Iizumi, K. Saiki, A. Koma, N.S. Sokolov, J. Electron Spectrosc. and Relat. Phenom. 88 (1998), p. 457

[8] R.F. Egerton, Electron Energy Loss Spectroscopy in the Electron Microscope, 2nd Edition, Plenum Press, New York (1996)

[9] J. Daniels, C.V. Festenberg, H. Raether, K. Zeppenfeld. Optical Constants of

Solids by Electron Spectroscopy. Springer Tracts in Modern Physics, Springer-Verlag, New York, (1970), Vol. 54, p. 78-135

[10] J. Pflüger, J. Fink, W. Weber, K.P. Bohnen, G. Crecelins, Phys. Rev. B 30 (1984), p.1155

[11] W.Y. Liang, A.R. Beal, J. Phys. C 9 (1976), p. 2823

[12] P. Blaha, K. Schwarz, G.K. H. Madsen, D. Kvasnicka and J. Luitz, Computer code WIEN2k (Technische Universität Wien, Austria, 2001)

[13] Claudia Ambrosch-Draxl, Jorge O. Soto, Computer Phys. Commun. 175 (2006), p. 175

[14] K. Ichinose, K. Fujiwara, H. Yoshie, H. Nagai, A. Tsujimura, J. Physical Society of Japan 55(4) (1986), p. 1336

[15] F. Espinosa-Magaña, A. Duarte-Moller, R. Martínez-Sánchez, M. Miki-Yoshida, J. Electron Spectrosc. Relat. Phenom. 125 (2002), p.119

[16] D.J. Singh, M. Gupta, Phys. Rev. B 69, (2001), p. 32403

[17] K.H.J. Buschow, A.M. van Diepen, Solid State Commun. 19, (1976), p. 79

[18] J.C. Crivello, M. Gupta, J. Alloys and Compounds 404-406, (2005), p. 150